Organometallic Catalysis in Aqueous Solution. The Hydrolytic Activity of a Water-Soluble *ansa*-Molybdocene Catalyst

Takiya J. Ahmed, Lev N. Zakharov, and David R. Tyler*

Department of Chemistry, University of Oregon, Eugene, Oregon 97403

Received May 10, 2007

The synthesis, characterization, and reactivity of the new water-soluble *ansa*-molybdocene catalyst [{$C_2Me_4(C_5H_4)_2$}Mo(OH)(OH_2)][OTs] (**3**) and the related hydroxo-bridged dimer [{$C_2Me_4(C_5H_4)_2$}Mo-(μ-OH)]$_2$[OTs]$_2$ (**5**) are described. The effect of the ethylene bridge on the metallocene structure was evaluated by comparing the crystal structures of {$C_2Me_4(C_5H_4)_2$}MoH_2 (**2**) and **5** to those of the non-*ansa* analogues. The ethylene bridge changed the bite angles of the metallocene fragment by only a few degrees in both *ansa* structures. To probe the electronic consequences of the tetramethylethylene bridge, the {$C_2Me_4(C_5H_4)_2$}Mo(CO)H (**4**) complex was prepared. On the basis of the ν(C≡O) stretching frequencies, the *ansa* ligand $C_2Me_4(C_5H_4)_2$ was found to be electron-withdrawing relative to two η^5-C_5H_5 ligands. The reactivity of **3** in nitrile hydration, phosphate ester hydrolysis, and carboxylic acid ester hydrolysis was explored, and the rate constants for these transformations were compared to rate constants obtained using the $Cp_2Mo(OH)(OH_2)^+$ and $Cp'_2Mo(OH)(OH_2)^+$ catalysts. In all cases, the Cp_2-$Mo(OH)(OH_2)^+$ catalyst, having intermediate electron density, had the largest rate constants. The reactivity trends for the three catalysts are explained by the relative electrophilicities of the Mo centers. If electron-donating cyclopentadienyl ligands are employed, the reactivity of the bound substrate is decreased relative to Cp and the rate is decreased. Conversely, if electron-withdrawing Cp cyclopentadienyl ligands are employed, the reactivity of the bound hydroxo nucleophile is decreased and the rate is decreased. In the case of the $Cp_2Mo(OH)(OH_2)^+$ complex, these two opposing trends converge, and optimal activity is observed.

Introduction

Molybdocenes containing aqua and hydroxo ligands are water-soluble, and several such complexes have been extensively used as catalysts and mediators in aqueous-phase reactions.[1−12] The $Cp_2Mo(OH)(OH_2)^+$ complex was the first organometallic complex reported to hydrolyze phosphate esters[7,10,11] at rates comparable to the excellent Co(III) amine hydrolysis catalysts studied by Chin et al.[13] Later investigations of the $Cp'_2Mo(OH)(OH_2)^+$ (Cp′ = η^5-C_5H_4Me) complex (Figure 1a) in our laboratory extended the utility of the molybdocenes to catalytic hydration[2,3] and H/D exchange reactions,[4−6] the latter being one of the few examples of C−H bond activation in water. Ongoing efforts to exploit molybdocenes for environmentally benign transformations of organic substrates have continued with an exploration of the electronic and steric effects of substituted cyclopentadienyl ligands on the reactivity of the molybdocenes. *ansa*-Ligands (bridged cyclopentadienyl rings; Figure 1b) offer a convenient method of altering the geometric structure and electronics of the cyclopentadienyl ligands without the use of substituents containing functional groups that may interfere with the catalyst active site.

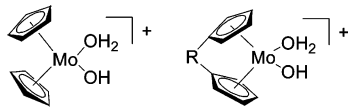

a. b.

Figure 1. Structures of (a) a water-soluble molybdocene catalyst and (b) a water-soluble *ansa*-molybdocene.

ansa-Bridges were shown to have a significant impact on the geometric structure, electronic structure, and reaction chemistry of molybdocenes.[14−26] Molecules with one-atom bridges (the type most commonly studied) significantly reduce

* Corresponding author. E-mail: dtyler@uoregon.edu.

(1) Breno, K. L.; Ahmed, T. J.; Pluth, M. D.; Balzarek, C.; Tyler, D. R. *Coord. Chem. Rev.* **2006**, *250*, 1141−1151.
(2) Breno, K. L.; Pluth, M. D.; Landorf, C. W.; Tyler, D. R. *Organometallics* **2004**, *23*, 1738−1746.
(3) Breno, K. L.; Pluth, M. D.; Tyler, D. R. *Organometallics* **2003**, *22*, 1203−1211.
(4) Breno, K. L.; Tyler, D. R. *Organometallics* **2001**, *20*, 3864−3868.
(5) Balzarek, C.; Tyler, D. R. *Angew. Chem., Int. Ed.* **1999**, *38*, 2406−2408.
(6) Balzarek, C.; Weakley, T. J. R.; Tyler, D. R. *J. Am. Chem. Soc.* **2000**, *122*, 9427−9434.
(7) Kuo, L. Y.; Barnes, L. A. *Inorg. Chem.* **1999**, *38*, 814−817.
(8) Kuo, L. Y.; Blum, A. P.; Sabat, M. *Inorg. Chem.* **2005**, *44*, 5537−5541.
(9) Kuo, L. Y.; Finigan, D. M.; Tadros, N. N. *Organometallics* **2003**, *22*, 2422−2425.
(10) Kuo, L. Y.; Kuhn, S.; Ly, D. *Inorg. Chem.* **1995**, *34*, 5341−5.
(11) Kuo, L. Y.; Perera, N. M. *Inorg. Chem.* **2000**, *39*, 2103−2106.
(12) Kuo, L. Y.; Weakley, T. J. R.; Awana, K.; Hsia, C. *Organometallics* **2001**, *20*, 4969−4972.
(13) Chin, J. *Acc. Chem. Res.* **1991**, *24*, 145−52.
(14) Churchill, D.; Shin, J. H.; Hascall, T.; Hahn, J. M.; Bridgewater, B. M.; Parkin, G. *Organometallics* **1999**, *18*, 2403−2406.
(15) Chernega, A.; Cook, J.; Green, M. L. H.; Labella, L.; Simpson, S. J.; Souter, J.; Stephens, A. H. H. *J. Chem. Soc., Dalton Trans.* **1997**, 3225−3243.
(16) Churchill, D. G.; Bridgewater, B. M.; Zhu, G.; Pang, K.; Parkin, G. *Polyhedron* **2006**, *25*, 499−512.
(17) Janak, K. E.; Shin, J. H.; Parkin, G. *J. Am. Chem. Soc.* **2004**, *126*, 13054−13070.
(18) Labella, L.; Chernega, A.; Green, M. L. H. *J. Chem. Soc., Dalton Trans.* **1995**, 395−402.
(19) Labella, L.; Chernega, A.; Green, M. L. H. *J. Organomet. Chem.* **1995**, *485*, C18−C21.

10.1021/om7004657 CCC: $37.00
Publication on Web 09/07/2007

Scheme 1. Proposed Mechanism of Intramolecular Hydroxide Attack

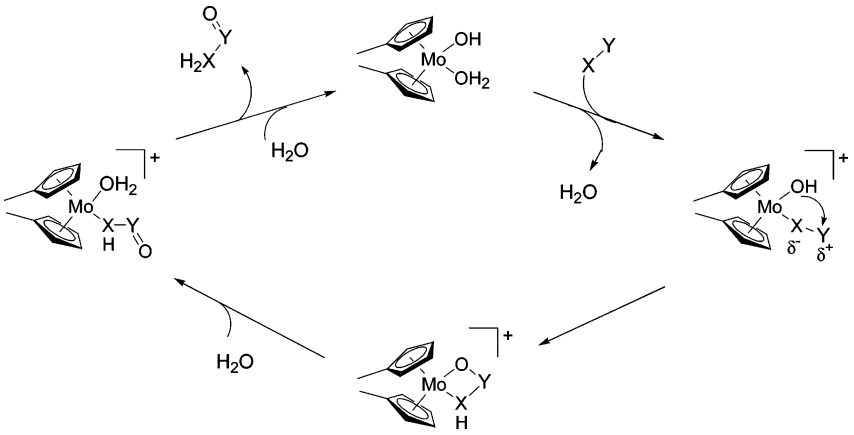

the bite angle of the metallocene moiety and enhance the bonding of the Cp rings to the metal center. The stronger Cp−M bonds in these molecules were recently shown to be the result of a more stable acceptor orbital on the Cp ligand with consequent increased back-donation from the metal center.[27] In a Mo(IV) metallocene, this results in an even more electrophilic metal center.[17]

The studies reported herein were conducted in order to investigate the reactivity of the more electrophilic metal center of *ansa* molybdocenes in aqueous-phase hydration and hydrolysis reactions. The general mechanism of $Cp^{(\prime)}_2Mo(OH)(OH_2)^+$-mediated hydrolysis ($Cp^{(\prime)} = \eta^5$-$C_5H_5$ or η^5-C_5H_4Me) is Lewis acid activation of the substrate followed by intramolecular attack of the coordinated hydroxo ligand (Scheme 1).[2] In prior studies, improved catalytic performance was noted for transformations of nitriles containing electron-withdrawing groups due to a greater positive charge on the electrophilic carbon center.[3] For similar reasons, it was postulated that a more electrophilic metal center might also lead to enhanced activation of the substrate and enhanced reactivity. Alternatively, a more electrophilic metal center will also influence the rate of attack by a coordinated nucleophile.

Other molecular parameters may influence the rate, as well. Investigations of Co(III)-,[13,28,29] Ir(III)-,[30] Cu(II)-,[31−35] and Zn-(II)-catalyzed[36−40] hydrolysis reactions that proceed by intramolecular nucleophilic attack demonstrated that the rate of hydrolysis can be affected by (1) the acidity of the protonated hydroxo nucleophile, (2) the tendency of the active catalyst to dimerize, and (3) steric changes that lead to stabilization of the cyclic intermediate. With regard to the first of these factors, note that the protonated nucleophile in water-soluble molybdocene complexes is relatively acidic ($pK_{a1} \approx 5.5$). Therefore, the expected decrease in the pK_a of the relatively electrophilic *ansa* complex is not expected to influence the concentration of the active catalyst or the reactivity of the molybdocene at neutral pH. As for the second factor, the tendency of the molybdocenes to dimerize may influence the rate of catalysis and must be taken into account. Last, because *ansa* linkages are known to alter the geometric structure of metallocenes, any structural changes in the *ansa* complex must be carefully analyzed to determine their significance.

In an initial study of how a more electrophilic molybdocene complex reacts toward intramolecular nucleophilic attack, the silyl-bridged *ansa*-molybdocene $[SiMe_2(C_5H_4)_2Mo(OH)(OH_2)][OTs]$ was studied.[1] Unfortunately, the Si−Cp bonds of $[SiMe_2(Cp_2Mo(OH)(OH_2)]^{2+}$ were unstable to hydrolysis, and an aqueous solution of the complex readily degraded to give the $[Cp_2Mo(OH)(OH_2)]^+$ and $[Cp_2Mo(\mu\text{-}OH)]_2^{2+}$ complexes. To avoid problems associated with the hydrolysis of C−Si bonds, the previously unexplored ethylene-bridged *ansa*-molybdocene $[\{C_2Me_4(\eta^5\text{-}C_5H_4)_2\}Mo(OH)(OH_2)][OTs]$ and its related binuclear analogue $[\{C_2Me_4(\eta^5\text{-}C_5H_4)_2\}Mo(\mu\text{-}OH)]_2[OTs]_2$ were prepared (Figure 2). In addition to being less susceptible to hydrolysis, the ethylene bridges were also chosen because they generally induce minimal structural changes in the bite angles and ring tilts of bent metallocenes,[27] thereby avoiding the large structural changes caused by one-atom *ansa* bridges. The changes in reactivity for an ethylene-bridged *ansa* catalyst, therefore, can be solely attributed to electronic changes at the metal center and not to steric changes. The results reported below expand our understanding of the reactivity of substituted molybdocenes as well as the general *ansa* effect in molybdocene systems. (In this paper, "substituted molybdocenes" refers to

(20) Pons, V.; Conway, S. L. J.; Green, M. L. H.; Green, J. C.; Herbert, B. J.; Heinekey, D. M. *Inorg. Chem.* **2004**, *43*, 3475−3483.
(21) Green, J. C.; Harvey, J. N.; Poli, R. *J. Chem. Soc., Dalton Trans.* **2002**, 1861−1866.
(22) Comte, V.; Blacque, O.; Kubicki, M. M.; Moiese, C. *Organometallics* **1997**, *16*, 5763−5769.
(23) Conway, S. L. J.; Dijkstra, T.; Doerrer, L. H.; Green, J. C.; Green, M. L. H.; Stephens, A. H. H. *J. Chem. Soc., Dalton Trans.* **1998**, 2689−2696.
(24) Jourdain, I. V.; Fourmigue, M.; Guyon, F.; Amaudrut, J. *Organometallics* **1999**, *18*, 1834−1839.
(25) Churchill, D. G.; Bridgewater, B. M.; Parkin, G. *J. Am. Chem. Soc.* **2000**, *122*, 178−179.
(26) Churchill, D. G.; Janak, K. E.; Wittenberg, J. S.; Parkin, G. *J. Am. Chem. Soc.* **2003**, *125*, 1403−1420.
(27) Zachmanoglou, C. E.; Docrat, A.; Bridgewater, B. M.; Parkin, G.; Brandow, C. G.; Bercaw, J. E.; Jardine, C. N.; Lyall, M.; Green, J. C.; Keister, J. B. *J. Am. Chem. Soc.* **2002**, *124*, 9525−9546.
(28) Chin, J.; Banaszczyk, M.; Jubian, V.; Zou, X. *J. Am. Chem. Soc.* **1989**, *111*, 186−90.
(29) Chin, J.; Zou, X. *J. Am. Chem. Soc.* **1988**, *110*, 223−5.
(30) Hendry, P.; Sargeson, A. M. *J. Am. Chem. Soc.* **1989**, *111*, 2521−7.
(31) Kou, X.; Cheng, S.; Du, J.; Yu, X.; Zeng, X. *J. Mol. Catal. A: Chem.* **2004**, *210*, 23−29.
(32) Hegg, E. L.; Mortimore, S. H.; Cheung, C. L.; Huyett, J. E.; Powell, D. R.; Burstyn, J. N. *Inorg. Chem.* **1999**, *38*, 2961−2968.
(33) Deal, K. A.; Burstyn, J. N. *Inorg. Chem.* **1996**, *35*, 2792−8.
(34) Deal, K. A.; Hengge, A. C.; Burstyn, J. N. *J. Am. Chem. Soc.* **1996**, *118*, 1713−18.
(35) Itoh, T.; Hisada, H.; Usui, Y.; Fujii, Y. *Inorg. Chim. Acta* **1998**, *283*, 51−60.
(36) Fujii, Y.; Itoh, T.; Onodera, K.; Tada, T. *Chem. Lett.* **1995**, 305−6.
(37) Bazzicalupi, C.; Bencini, A.; Berni, E.; Bianchi, A.; Fedi, V.; Fusi, V.; Giorgi, C.; Paoletti, P.; Valtancoli, B. *Inorg. Chem.* **1999**, *38*, 4115−4122.
(38) Bonfa, L.; Gatos, M.; Mancin, F.; Tecilla, P.; Tonellato, U. *Inorg. Chem.* **2003**, *42*, 3943−3949.
(39) Itoh, T.; Fujii, Y.; Tada, T.; Yoshikawa, Y.; Hisada, H. *Bull. Chem. Soc. Jpn.* **1996**, *69*, 1265−1274.
(40) Koike, T.; Kimura, E. *J. Am. Chem. Soc.* **1991**, *113*, 8935−41.

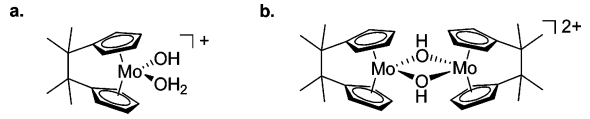

Figure 2. (a) Water-soluble ethylene-bridged molybdocene catalyst [{$C_2Me_4(\eta^5$-$C_5H_4)_2$}Mo(OH)(OH_2)][OTs] and (b) its binuclear analogue [{$C_2Me_4(\eta^5$-$C_5H_4)_2$}Mo(μ-OH)]$_2$[OTs]$_2$.

substitution on the cyclopentadienyl rings. Likewise, "unsubstituted" refers to a molecule with η^5-C_5H_5 rings.)

Experimental Section

General Procedures. All experiments were performed under a nitrogen atmosphere using a glovebox or a Schlenk line. All solvents were dried and distilled from appropriate drying agents. Solvents and substrates were then purged with nitrogen or degassed using three freeze−pump−thaw cycles. Solutions buffered to pD 6.8 were prepared by dissolving *N*-morpholinopropylsulfonic acid (MOPS) hemisodium salt in D_2O. The compounds $C_2Me_4(C_5H_4MgCl)_2$,[41] $MoCl_4$·dme,[42] [$Cp_2Mo(\mu$-OH)]$_2$[OTs]$_2$,[43] and [$Cp'_2Mo(\mu$-OH)]$_2$-[OTs]$_2$[44] were prepared as described in the literature.

All hydrolysis and hydration reaction samples were prepared in a glovebox under an atmosphere of N_2 in Wilmad 9 in. precision NMR tubes or Wilmad J-Young screw cap NMR tubes. Reactions carried out in the Wilmad 9 in. NMR tubes were flame sealed while frozen. Reaction tubes were heated in an oil bath. ^{1}H NMR spectra were obtained using a Varian Inova 500 MHz (500.104 MHz for ^{1}H and 125.764 MHz for ^{13}C) or 600 MHz NMR spectrometer (599.982 MHz for ^{1}H and 150.879 MHz for ^{13}C). ^{1}H NMR resonances were integrated relative to the 7.657 ppm tosylate peak from the catalyst counterion or to the 2.10 ppm MOPS buffer resonance. Phosphate ester hydrolysis was monitored using a Hewlett-Packard 8453 UV/vis spectrophotometer. IR spectra were obtained using a Nicolet Magna IR 530 spectrometer.

Synthesis of [{$C_2Me_4(\eta^5$-$C_5H_4)_2$}$MoCl_2$] (1). The following preparation was adapted from that reported by Green et al.[23] for the analogous tungsten complex. Approximately 300 mL of Et_2O was added to a previously stirred mixture of $MoCl_4$·dme (7.8 g, 24 mmol) and $C_2Me_4(C_5H_4MgCl)_2$ (15 g, 24 mmol) to obtain a grayish-brown suspension. After 3 days, the solvent was removed from the red-brown suspension in vacuo, leaving a pale, pink-brown solid that was extracted with toluene in a Soxhlet apparatus for 24 h. The toluene was removed under reduced pressure, and the red-brown solid was washed with hexanes to yield 2.3 g (26%) of {C_2-$Me_4(\eta^5$-$C_5H_4)_2$}$MoCl_2$ as a fine brown powder. ^{1}H NMR ($CDCl_3$): δ 6.14 (m, 4, C_5H_4), 5.84 (m, 4, C_5H_4), 1.00 (s, 12, C_2Me_4). ^{13}C-{^{1}H} NMR ($CDCl_3$): δ 127.59 (s, C_5H_4, C_{ipso}), 122.41 (s, C_5H_4), 82.95 (s, C_5H_4), 45.89 (s, C_2Me_4), 27.45(C_2Me_4). Anal. Found: C, 52.53; H, 5.87; Cl, 17.61. Calcd for $C_{16}H_{20}Cl_2Mo$·0.20 C_7H_8: C, 52.56; H, 5.48; Cl, 17.83.

Synthesis of [{$C_2Me_4(\eta^5$-$C_5H_4)_2$}MoH_2] (2). A suspension of $NaBH_4$ (0.80 g, 21 mmol) in THF was added to a solution of **1** (2.0 g, 5.3 mmol) in THF dropwise at −78 °C. The brown suspension was allowed to warm to room temperature and stirred overnight. After removing the THF under reduced pressure, the orange solid was extracted into benzene and pumped to dryness, leaving an oily, orange solid. The [{$C_2Me_4(\eta^5$-$C_5H_4)_2$}MoH_2] thus obtained (0.850 g, 52%) was not purified further but immediately used to generate complexes **3** and **5**, as described in the next section. However, compound **2** may be sublimed at 110 °C at 1 Torr, but this decreases the yield considerably. The ^{1}H and ^{13}C NMR spectra for **2** are provided in the Supporting Information and show the material obtained by sublimation is spectroscopically pure. ^{1}H NMR (C_6D_6): δ 4.92 (m, 4, C_5H_4), 4.69 (m, 4, C_5H_4), 0.75 (s, 12, C_2-Me_4), −6.88 (2, s, MoH_2). ^{13}C{^{1}H} NMR (THF-d_8): δ 106.82 (s, C_5H_4, C_{ipso}), 82.99 (s, C_5H_4), 72.94 (s, C_5H_4), 46.32 (s, C_2Me_4), 27.23 (C_2Me_4). IR (Nujol mull): 1774 cm^{-1} (ν(Mo−H)).

Synthesis of [{$C_2Me_4(\eta^5$-$C_5H_4)_2$}$Mo(\mu$-OH)]$_2$[OTs]$_2$ (5). This synthesis was adapted from the preparation of [Cp′2Mo(μ-OH)]$_2$-[OTs]$_2$.[44] A solution of *p*-toluenesulfonic acid monohydrate (0.48 g, 2.5 mmol) in acetone/water (70 mL/0.70 mL) was added to the orange solid (0.850 g, 2.7 mmol) obtained by the preceding description. The orange-red solution was refluxed for 8 h, during which time a gray-green suspension formed. The solvent was removed under reduced pressure to leave a light brown-gray solid that was rinsed with benzene and hexanes. As discussed in the Results and Discussion section, this procedure, which with non-*ansa* Cp ligands gives dimer complexes of the type [$Cp_2Mo(\mu$-OH)]$_2$[OTs]$_2$, instead gives **3** as the major product when using the *ansa*-$C_2Me_4(\eta^5$-$C_5H_4)_2$ ligand (0.73 g, 57% based on all monomer product). In this instance, the dimeric complex [{$C_2Me_4(\eta^5$-$C_5H_4)_2$}-Mo(μ-OH)]$_2$[OTs]$_2$ (**5**) formed only as a minor product. Attempts to purify **3** by crystallization yielded pure [{$C_2Me_4(\eta^5$-$C_5H_4)_2$}-Mo(μ-OH)]$_2$[OTs]$_2$ (**5**). Specifically, upon standing for 2−3 days, a saturated solution of **3** yielded green crystals of **5** as the dihydrate. (The water molecules could be readily removed by heating under reduced pressure.) Anal. Found for **5**: C, 55.78; H, 5.79; S, 6.22. Calcd for $C_{23}H_{28}SO_4Mo$: C, 55.64; H 5,68; S, 6.46. Data for **3**: ^{1}H NMR (DMSO): δ 7.71 (d, 2, *p*-OTs), 7.32 (d, 2, *p*-OTs), 6.95-(m, 4, C_5H_4), 6.00 (m, 4, C_5H_4), 2.29 (s, 3, *p*-OTs-Me), 0.726 (s, 12, C_2Me_4). ^{13}C{^{1}H} NMR (D_2O): δ 142.70 (s, *p*-OTs), 139.60 (s, *p*-OTs), 132.99 (s, C_5H_4, C_{ipso}), 129.65 (s, *p*-OTs), 125.57 (*p*-OTs), 119.89 (s, C_5H_4), 84.73 (s, C_5H_4), 43.73 (s, C_2Me_4) , 26.17 (s, C_2Me_4), 20.67 (s, *p*-OTs-Me). Data for **5**: ^{1}H NMR (DMSO): δ 7.71 (d, 2, *p*-OTs), 7.32 (d, 2, *p*-OTs), 7.45(m, 4, C_5H_4), 7.07 (m, 4, C_5H_4), 6.13 (m, 4, C_5H_4), 5.99 (m, 4, C_5H_4), 2.29 (s, 3, *p*-OTs-Me), 0.689 (s, 24, C_2Me_4).

Generation of [{$C_2Me_4(C_5H_4)_2$}Mo(CO)H][OTs] (4). A J-Young tube containing 0.5 mL of 0.5 mM **3** in D_2O was charged with 20 psi CO. After heating at 90 °C for 12 h, the D_2O was removed under reduced pressure, $CDCl_3$ was immediately added, and the ^{1}H NMR and IR spectra were obtained. ^{1}H NMR ($CDCl_3$): δ 7.87 (d, 2, *p*-OTs), 7.17 (d, 2, *p*-OTs), 6.35(m, 2, C_5H_4), 6.23 (m, 2, C_5H_4), 5.75 (m, 2, C_5H_4), 5.12 (m, 2, C_5H_4), 2.35 (s, 3, *p*-OTs-Me), 1.29 (d, 12, C_2Me_4), −7.29 (s, 1, Mo−H). IR ($CDCl_3$): 2028 cm^{-1} (ν(C≡O)).

X-ray Structure Determinations of [{$C_2Me_4(\eta^5$-$C_5H_4)_2$}MoH_2] (2) and [{$C_2Me_4(\eta^5$-$C_5H_4)_2$}$Mo(\mu$-OH)]$_2$[OTs]$_2$·2H_2O (5). Crystals suitable for X-ray diffraction analysis were grown by slow evaporation of benzene solutions of **2** and saturated aqueous solutions of **3**. X-ray diffraction experiments were carried out on a Bruker Smart Apex diffractometer at 173 K (**2**) or 150 K (**5**) using Mo Kα radiation (λ = 0.71070 Å). Absorption corrections were done by SADABS. Crystallographic data for **2** and **5** and the details of data collection and refinement of the crystal structures are given in the Supporting Information. The structures were solved using direct methods and refined with full-matrix least-squares methods based on F^2. All non-H atoms were refined with anisotropic thermal parameters. The H atoms coordinated to the Mo atom in **2** and all H atoms in **5** were found on the F-map and refined with isotropic thermal parameters. Other H atoms in **2** were treated in calculated positions and refined in a rigid group model. It should be mentioned that on the residual density of **2** there are two relatively high peaks, 6.04 and 4.53 e·Å^{-3}. The distances from the Mo(1) atoms and these peaks are about 1.6 Å, and they form with the Mo atom a linear fragment with an angle 177°. Attempts to remove these two peaks by changing absorption corrections failed. Data collection with two

(41) Schwemlein, H.; Brintzinger, H. H. *J. Organomet. Chem.* **1983**, *254*, 69−73.
(42) Persson, C.; Andersson, C. *Inorg. Chim. Acta* **1993**, *203*, 235−8.
(43) Ren, J. G.; Tomita, H.; Minato, M.; Osakada, K.; Ito, T. *Chem. Lett.* **1994**, 637−40.
(44) Balzarek, C.; Weakley, T. J. R.; Kuo, L. Y.; Tyler, D. R. *Organometallics* **2000**, *19*, 2927−2931.

different crystals of **2** were done, and in both cases such peaks were found. Crystals of **2** are extremely unstable in air, and the existence of these peaks seems to be related to a small amount of decomposition during crystal mounting on the diffractometer. All calculations were performed using the SHELXTL package.

Crystals of **5** have two polymorphic phases, and the structures of both of them were determined (see Supporting Information). Both structures have the same dimeric Mo units and tosylate as counterions, but the structural function of a solvent water molecule is different. In **5**, the μ-OH groups of the dimeric Mo hydrogen bond to the O atoms of the OTs counterions (Figure 5). In the second polymorph, the μ-OH groups form hydrogen bonds with the solvent water molecules, which form a further hydrogen-bonding network with the tosylate anions.

Preparation of Catalyst Stock Solutions. Stock solutions of **3**, $[Cp_2Mo(OH)(OH_2)][OTs]$, and $[Cp'_2Mo(OH)(OH_2)][OTs]$ were prepared by dissolving crystals of the respective dimeric complex **5**, $[Cp_2Mo(\mu\text{-}OH)_2]_2[OTs]_2$, or $[Cp'_2Mo(\mu\text{-}OH)_2]_2[OTs]_2$ in 0.13 M MOPS-buffered D_2O to give solutions ranging from 2 to 15 mM total molybdenum concentration ($[Mo]_{total}$). The total molybdenum concentration in each solution was determined using a known amount of tetrabutylammonium tetrafluoroborate as an internal standard. The catalyst concentration for the non-*ansa* catalysts was calculated from the total molybdenum concentration using the relationships $[Mo]_{total} = [OTs^-] = 2[dimer] + [monomer]$ and $K_{eq} = [monomer]^2/[dimer]$. (As will be discussed below, the active monomeric catalyst is in equilibrium with an inactive dimeric species.) In the case of the *ansa* catalyst, $[Mo]_{total} = [OTs^-] = [monomer]$.

Nitrile Hydration. 3-Hydroxypropionitrile (3−10 μL) was added to 0.50 mL of catalyst solution. The tube was then heated to 80 °C for 14 days. Addition of 3-HPN caused the stock solution of $[Cp'_2Mo(OH)(OH_2)][OTs]$ to turn pink, while the other two solutions remained yellow. ^{1}H NMR spectroscopy (D_2O) was used to monitor the disappearance of 3-hydroxypropionitrile at 3.78 ppm (t, J = 6.0 Hz, 2H, $HOCH_2CH_2CN$) and 2.67 ppm (t, J = 6.0 Hz, 2H, $HOCH_2CH_2CN$) and the appearance of 3-hydroxypropionamide at 3.76 ppm (t, J = 6.0 Hz, 2H, $HOCH_2CH_2CONH_2$) and 2.45 ppm (t, J = 6.0 Hz, 2H, $HOCH_2CH_2CONH_2$).

***p*-Nitrophenyl Phosphate Hydrolysis.** The appropriate catalyst solution (2 mL) was added to a nitrogen-filled cuvette and placed in a water bath heated to 30 °C. After 30 min, a 20 μL aliquot of 0.45 mM NPP was added to the catalyst solution. The production of *p*-nitrophenolate anion was monitored at 400 nm until no further change in absorbance was observed.

Ethyl Acetate Hydrolysis. Ethyl acetate (5−20 μL) was added to 0.50 mL of the catalyst stock solutions and heated to 80 °C for 7−9 days. The reaction was monitored by the disappearance of ester ^{1}H NMR resonances (500 MHz, D_2O) at 4.05 ppm (q, J = 7.0 Hz, 2H, $CH_3CO_2CH_2CH_3$), 1.96 ppm (s, 3H, $CH_3CO_2CH_2CH_3$), and 1.15 ppm (t, J = 7.0 Hz, 2H, $CH_3CO_2CH_2CH_3$) and the appearance of ethanol and acetic acid at 3.55 ppm (q, J = 7.0 Hz, 2H, $HOCH_2CH_3$), 1.08 ppm (t, J = 7.0 Hz, 3H, $HOCH_2CH_3$), and 1.95 (s, 3H, CH_3CO_2H).

Equilibrium Constant Determinations. Solutions containing various concentrations of $[Cp_2Mo(\mu\text{-}OH)]_2[OTs]_2$ and $[Cp'_2Mo(\mu\text{-}OH)]_2[OTs]_2$ were prepared using a 0.13 M MOPS D_2O solution. The concentrations of monomer and dimer were determined by integrating the respective Cp ^{1}H NMR resonances relative to the OTs resonance at 7.657 ppm. For Cp_2Mo^{2+}, the dimer resonance at 5.929 ppm decreased relative to the monomer resonance at 5.724 ppm with decreasing total molybdocene concentration. For Cp'_2Mo^{2+}, the dimer resonances at 5.904 and 5.623 ppm decreased relative to the monomer resonances at 5.389 and 5.352 ppm with decreasing total molybdocene concentration. Samples used for the determinations at 80 °C were preheated in an oil bath for 1 h before insertion into a 600 MHz NMR spectrometer preheated to 80 °C. In all cases, the proton chemical shifts were referenced to residual HOD, and the chemical shifts at 80 °C are shifted slightly downfield. At 80 °C, the Cp resonance for $[Cp_2Mo(\mu\text{-}OH)]_2[OTs]_2$ appears at 6.384 ppm, and $[Cp_2Mo(OH)(OH_2)][OTs]$ shifts to 6.187 ppm. Likewise, at 80 °C, the $[Cp'_2Mo(\mu\text{-}OH)]_2[OTs]_2$ resonances appear at 6.345 and 6.038 ppm, and $[Cp'_2Mo(\mu\text{-}OH)(OH)_2][OTs]$ resonances appear at 5.926 and 5.775 ppm.

Results and Discussion

Aqueous Solubility and Behavior of Molybdocenes. The aqueous solubility of Cp_2MoX_2-type molecules is attributed to spontaneous and rapid hydrolysis of the Mo−X bonds to afford ionic complexes containing inner-sphere aqua and hydroxo ligands that are capable of hydrogen bonding. The aquated molybdocene $Cp_2Mo(OH_2)^{2+}$ was found to have pK_a values of 5.5 and 8.5.[45] Of the aquated species generated by hydrolysis of Cp_2MoX_2, the $Cp_2Mo(OH)(OH_2)^+$ cation present at neutral pH was shown to be catalytically most active.[6,10] However, in a previous study, the monomer species were shown to be in equilibrium with the inactive μ-hydroxo dimer $[Cp_2Mo(\mu\text{-}OH)]_2^{2+}$ (eq 1).[44] The equilibrium constants for the reactions in eq 1 were determined to be $(3.5 \pm 0.1) \times 10^{-2} \times 10^{-2}$ M and $(7.9 \pm 0.1) \times 10^{-2}$ M for R = H at pH 3.5 and R = Me at pH 7, respectively. Comparison of these values indicates that the addition of a methyl substituent to each Cp ring shifts the monomer−dimer equilibrium in favor of the monomer. However, the equilibria were measured at different pH values. Because the equilibrium processes are sensitive to pH, for the accurate interpretation of the kinetic data it was necessary to measure K_{eq} for both systems under the conditions used for the catalysis reactions discussed below.

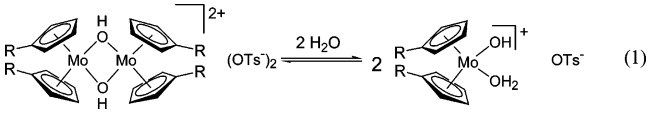

(1)

The equilibria in 0.13 M MOPS D_2O solutions (pD 6.8) at 25 and 80 °C were investigated by determining the change in the monomer and dimer concentrations in solutions containing various concentrations of total molybdocene. The respective monomer and dimer concentrations were plotted as $[monomer]^2$ versus [dimer] and are shown in Figure 3. From these data, the equilibrium constants, the changes in standard enthalpy, and the changes in standard entropy were calculated (Table 1). Consideration of the standard enthalpy and entropy changes gives some insight into the effect of adding a methyl substituent to each Cp ring. With both equilibria, formation of the monomer is enthalpically disfavored, roughly indicating that the Mo−OH bonds in the dimer are stronger than the Mo−OH_2 bonds in the monomer. Stronger solvation of the dicationic dimer species compared to the monocationic monomer will also contribute to the positive $\Delta H°$. However, the $\Delta H°$ is 4.7 kcal/mol smaller for the equilibrium with the Cp′ ligand versus the unsubstituted Cp ligand. This result indicates that the stability gained through dimerization of $[Cp'_2Mo(OH)(OH_2)][OTs]$ is much less than that gained through dimerization of $[Cp_2Mo(OH)(OH_2)][OTs]$, consistent with a decrease in the Lewis acidity of the metal center in Cp'_2Mo^{2+}. The decreased stability

(45) Kuo, L. Y.; Kanatzidis, M. G.; Sabat, M.; Tipton, A. L.; Marks, T. J. *J. Am. Chem. Soc.* **1991**, *113*, 9027−45.
(46) Schultz, A. J.; Stearley, K. L.; Williams, J. M.; Mink, R.; Stucky, G. D. *Inorg. Chem.* **1977**, *16*, 3303−6.
(47) Ren, J.-G.; Tomita, H.; Minato, M.; Ito, T.; Osakada, K.; Yamasaki, M. *Organometallics* **1996**, *15*, 852−9.

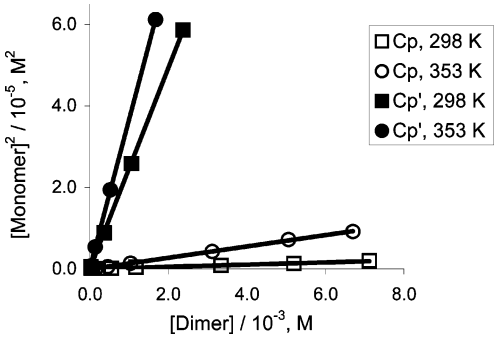

Figure 3. Plots of $([CpR_2Mo(OH)(OH_2)][OTs])^2$ versus $[CpR_2Mo(\mu\text{-}OH)]_2[OTs]_2$ in 0.13 M MOPS D_2O solution (pD 6.8). For R = H, (□) $K_{eq} = (2.7 \pm 0.1) \times 10^{-4}$ M at 25 °C and (○) $K_{eq} = (1.4 \pm 0.2) \times 10^{-3}$ M at 80 °C. For R = Me, (■) $K_{eq} = (2.5 \pm 0.1) \times 10^{-2}$ M at 25 °C and (●) $K_{eq} = (3.7 \pm 0.3) \times 10^{-2}$ M at 80 °C.

of the Mo−OH bonds in $[Cp'_2Mo(\mu\text{-}OH)]_2^{2+}$ may also be due to unfavorable steric interactions between the Cp′ methyl substituents on dimerization.

The hydrolysis of $[Cp_2Mo(\mu\text{-}OH)]_2[OTs]_2$ is entropically favored, but the hydrolysis of $[Cp'_2Mo(\mu\text{-}OH)]_2[OTs]_2$ is entropically disfavored (Table 1). Because hydrolysis of the dimer can superficially be described as three molecules reacting to give two, $\Delta S°$ was expected to be negative. On the other hand, conversion of the dication into two monocations should lead to a positive $\Delta S°$ because less solvent ordering is involved in solvating the less charged monomeric molecule. Accordingly, one may conclude that the latter factor is most important in determining the entropy in the hydrolysis of $[Cp_2Mo(\mu\text{-}OH)]_2[OTs]_2$, where $\Delta S°$ is positive. The addition of the methyl substituent decreases the solvation energy of the dimer, with a concomitant decrease in importance of the molecular charge and solvent order. In this case, the former factor apparently dominates, and the entropy of the system decreases because the dimer reacts with two water molecules to give two monomeric species.

In summary, the addition of a methyl substituent to the Cp rings shifts the monomer−dimer equilibrium in favor of the monomer because the Mo−OH bonds of $[Cp'_2Mo(\mu\text{-}OH)]_2[OTs]_2$ are weaker due to the decreased electrophilicity of the metal center and because of unfavorable steric interactions between the methyl groups. Because of the negative $\Delta S°$, formation of the $Cp'Mo(OH)(OH_2)^+$ monomer becomes less favorable at elevated temperature.

Synthesis of $[\{C_2Me_4(C_5H_4)_2\}Mo(OH)(OH_2)][OTs]$: Effect of the Ethylene Bridge on Aqueous Solubility and Behavior. The *ansa* ligand had at least four effects on the behavior of molybdocenes in water. First, the $[\{C_2Me_4(C_5H_4)\}MoCl_2]$ complex exhibited different behavior in water from other Cp_2MoX_2-type complexes in that it did not undergo hydrolysis. The water-soluble *ansa* complexes were, therefore, accessed from the dihydrido compounds $\{C_2Me_4(C_5H_4)_2\}MoH_2$ via hydrogenation of acetone in the presence of trace water in acetone solvent (eq 2).

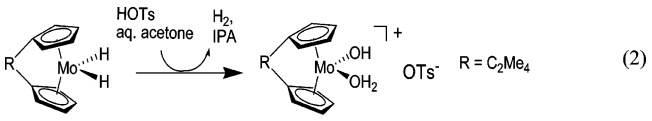

(2)

Second, although the route in eq 2 has been used previously for direct access to the dimeric structure $[Cp_2^{(\prime)}Mo(\mu\text{-}OH)]_2^{2+}$,[43,44] the reaction using the $\{C_2Me_4(C_5H_4)_2\}MoH_2$ complex produces

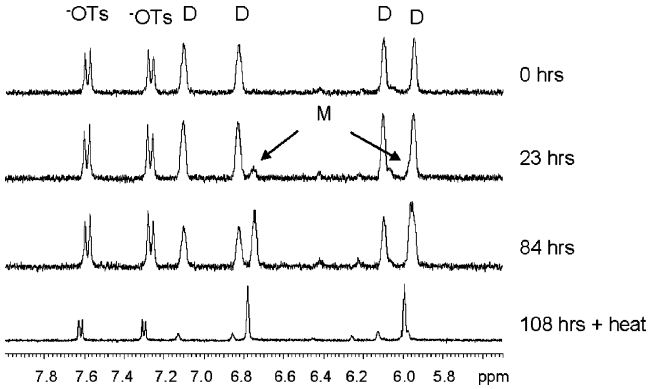

Figure 4. ^1H NMR spectra showing hydrolysis of $[\{C_2Me_4(C_5H_4)_2\}Mo(\mu\text{-}OH)]_2$ (D) to give $[C_2Me_4Co_2Mo(OH)(OH_2)]^+$ (M). OTs^- denotes the tosylate counterion resonances.

Table 1. Equilibrium Constants and Standard Thermodynamic Parameters for the Equilibrium in Eq 1 in 0.13 M MOPS Buffer (pH 6.8)

	R = H	R = Me
K_{eq} at 25 °C (M)	$(2.7 \pm 0.1) \times 10^{-4}$	$(2.5 \pm 0.1) \times 10^{-2}$
K_{eq} at 80 °C (M)	$(1.4 \pm 0.2) \times 10^{-3}$	$(3.7 \pm 0.3) \times 10^{-2}$
$\Delta H°$ (kcal/mol)	6.2 ± 0.5	1.5 ± 0.1
$\Delta S°$ (eu)	4.3 ± 0.3	-2.3 ± 0.2

the monomeric $[C_2Me_4Cp_2Mo(OH)(OH_2)]^+$ as the major product and the dimeric $[C_2Me_4Cp_2Mo(\mu\text{-}OH)]_2[OTs]_2$ only as a minor product. The dimeric $[C_2Me_4Cp_2Mo(\mu\text{-}OH)]_2[OTs]_2$ species was also generated in solution by dissolving $[C_2Me_4Cp_2Mo(OH)(OH_2)]^+$ in aqueous methanol. This yielded a mixture of monomer and dimer. To obtain pure, solid $[C_2Me_4Cp_2Mo(\mu\text{-}OH)]_2[OTs]_2$, the dimer was crystallized from a supersaturated solution of $[C_2Me_4Cp_2Mo(OH)(OH_2)]^+$ in water or water was removed at reduced pressure from a solution of $[C_2Me_4Cp_2Mo(OH)(OH_2)]^+$. Once obtained by either of these methods, the dimer will readily undergo hydrolysis in water to afford the monomer, as shown by the ^1H NMR spectra in Figure 4. Third, no monomer−dimer equilibrium in D_2O was detectable by ^1H NMR spectroscopy. Last, the water solubility of the molybdocene is greatly reduced upon addition of the tetramethylethylene linkage. The impact of this decreased solubility is shown by the fact that the hydrolysis and hydration reactions discussed below were performed using solutions of $C_2Me_4Cp_2Mo(OH)(OH_2)^+$ that were less than 3 mM, whereas solutions of $Cp_2Mo(OH)(OH_2)^+$ and $Cp'_2Mo(OH)(OH_2)^+$ were up to 15 mM in total molybdenum concentration. Further investigations of the aqueous behavior of the $C_2Me_4Cp_2Mo(OH)(OH_2)^+$ catalyst are ongoing and will be discussed in more detail in a subsequent paper.

Effect of the Ethylene Bridge on the Geometric Structure of Molybdocenes. Crystal structures of $C_2Me_4Cp_2MoH_2$ (**2**) and $[C_2Me_4Cp_2Mo(\mu\text{-}OH)]_2[OTs]_2$ (**5**) are shown in Figures 5 and 6, respectively. In both structures, the cyclopentadienyl rings adopt an eclipsed conformation enforced by the bridging atoms. In the structure of $C_2Me_4Cp_2MoH_2$, the bite angle and Mo−Cp bond distances are only slightly reduced from the unsubstituted dihydride molecule (Table 2). In contrast, the methylene-bridged molybdocene prepared by Labella et al. has a bite angle reduced by ~20°.[18] The Mo−H bond distances are essentially equal in all three molecules. More importantly, the *ansa*-molybdocene dimer **5**, shown in Figure 6, is essentially isostructural to that of the nonbridged analogues, $[(C_5H_5)_2Mo(\mu\text{-}OH)]_2[OTs]_2$ and $[(C_5H_4Me)_2Mo(\mu\text{-}OH)]_2[OTs]_2$. Each molybdocene center exhibits a distorted pseudo-tetrahedral environment (counting the $Mo-Cp_{centroid}$ as a single "coordination" site) with bridging

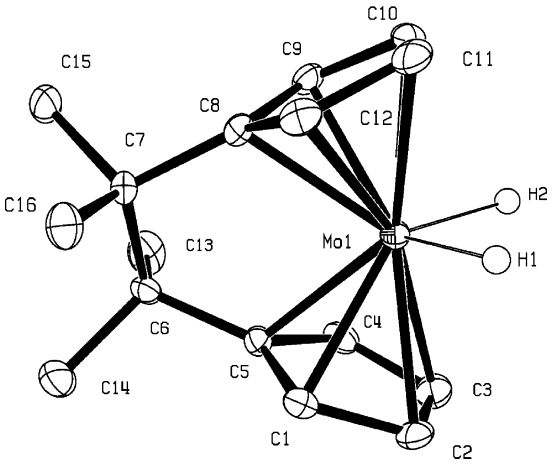

Figure 5. X-ray crystal structure of $(C_2Me_4Cp_2)MoH_2$. The Cp and bridge protons were omitted for clarity. Thermal ellipsoids are drawn at the 50% probability level.

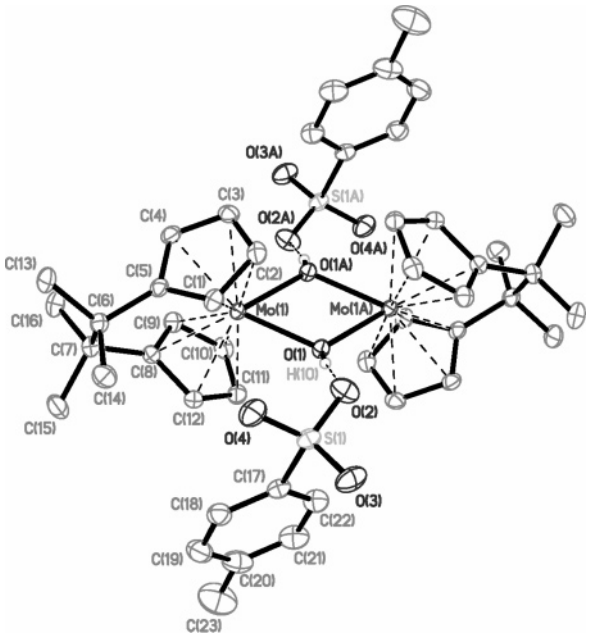

Figure 6. X-ray crystal structure of $[\{C_2Me_4(C_5H_4)_2\}Mo(\mu\text{-}OH)]_2[OTs]_2$ (**5**). The H atoms were omitted for clarity. Thermal ellipsoids are drawn at the 50% probability level.

hydroxo ligands hydrogen-bonded to the tosylate counterions. A comparison of selected angles and bond lengths is shown in Table 3. Note that there are only marginal variations in the geometric parameters for the Mo−O−Mo−O core, the bite angles, and $Cp_{centroid}$−Mo distances.

Table 4. Comparison of Selected Spectral Data for $Cp_2Mo(IV)$ Carbonyl Compounds

compound	C≡O (cm^{-1})	δ Mo−H	ref
$(C_5H_4Me)_2Mo(CO)H$	2008[a]	−8.09[b]	2
$(C_5H_5)_2Mo(CO)H$	2020[c]		48
$\{C_2Me_4(C_5H_4)_2\}Mo(CO)H$	2028[d]	−7.29[d]	this work

[a] KBr pellet. [b]$(CD_3)_2CO$. [c]$CHCl_3$. [d]$CDCl_3$.

Effect of the Ethylene Bridge on the Electronic Structure. In order to determine the effect of the ethylene bridge on the electron density of the Mo center, the CO-containing $[\{C_2Me_4(C_5H_4)_2\}Mo(CO)H][OTs]$ complex was prepared with the idea of using the ν(C≡O) frequency as a probe. The complex was prepared using the method previously reported for the Cp′ analogue (eq 3). Note that other synthetic routes to the $Cp_2Mo(CO)H^+$ complex are reported in the literature. In those routes, the carbonyl complex was generated by the oxidation of Cp_2MoCO using $CpMoH(CO)_3$ (eq 4) or by reduction of Cp_2MoH_2 with $[CpMo(CO)_3]_2$ in the presence of CO (eq 5).[48] Selected spectroscopic data for the various CO-containing molybdocenes are shown in Table 4. Comparison of the carbonyl stretching frequencies reveals that the ethylene-bridged molybdocene is relatively electron-withdrawing, as indicated by the C≡O stretch at highest frequency, followed by $Cp_2Mo(CO)(H)^+$ and $Cp'_2Mo(CO)H^+$. Note that this trend indicates that the electronic effect of the ethylene bridge is not inductive (as is the case in the $Cp'_2Mo(CO)H^+$ complex containing nonbridging methyl substituents). Instead, it is logical to propose that the electron-withdrawing nature of the *ansa* bridge is caused by enhanced back-donation into a relatively low-energy bis(cyclopentadienyl) ligand acceptor orbital, as explained by Parkin, Green, and co-workers in their comprehensive study of *ansa*-zirconocene complexes.[27]

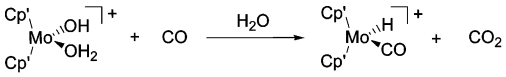

(3)

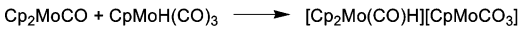

(4)

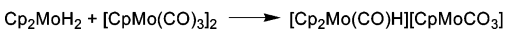

(5)

Effect of the Ethylene Bridge on Catalysis. To explore the effect of the more electrophilic molybdocene center in $C_2Me_4Cp_2Mo(OH)(OH_2)^+$ in reactions proceeding via intramolecular

Table 2. Comparison of Selected Bond Distances and Angles for the Molybdocene Dihydrides

ligand	Cp−Mo−Cp (deg)	H−Mo−H (deg)	Cp−Mo (Å)	H−Mo (Å)	ref
$(C_5H_5)_2$	145.8	75.5(3)	1.942, 1.946	1.685(3)	46
$\{C_2Me_4Cp_2\}$	141.9	85(3)	1.936, 1.933	1.68(7), 1.70(6)	this work
$\{CMe_2Cp_2\}$	121	80.3	1.913, 1.912	1.66(5), 1.72(7)	18

Table 3. Comparison of Selected Bond Distances and Angles for the Molybdocene Dimers

		$[\{(C_5H_4R)_2\}Mo(\mu\text{-}OH)]_2[OTs]_2$	
	$[\{C_2Me_4(C_5H_4)_2\}Mo(\mu\text{-}OH)]_2[OTs]_2$	R = H[a]	R = Me[b]
Mo−O	2.101(1)	2.092(2)	2.106(3)
Mo−O(1A)	2.112(1)	2.100(2)	2.095(3)
Mo−Cp(1)[c]	1.983	2.001(5)	2.001(3)
Mo−Cp(2)[c]	1.984	1.996(5)	1.997(3)
O(1)−Mo−(O1A)	66.90(5)	66.21(10)	67.0(1)
Mo1−O(1)−Mo1A	113.10(5)	113.79(10)	113.0(1)
Cp(1)−Mo−Cp(2)[c]	129.6	128.3	130.0

[a] Ref 47. [b]Ref 44. [c]Distances and angles are to the centroid of the Cp rings.

hydroxide attack, three reactions were investigated: (1) the hydration of 3-hydroxypropionitrile (HPN); (2) the hydrolysis of *p*-nitrophenyl phosphate (NPP); and (3) the hydrolysis of ethyl acetate (EtOAc). As explained in the Introduction, the electron-withdrawing *ansa*-Cp ligand could lead to enhanced activation of a bound substrate; however, it could also reduce the reactivity of the coordinated hydroxo nucleophile. To investigate the relative importance of these two competing factors, the rate constants for the reactions above catalyzed by the relatively electron poor *ansa*-molybdocene complex **3** were compared to those of the nonsubstituted molybdocene complex $Cp_2Mo(OH)(OH_2)^+$ and to the relatively electron-rich $Cp'_2Mo(OH)(OH_2)^+$ catalyst. All reactions were performed in 0.13 M MOPS-buffered D_2O with less than 3% catalyst. The rate constants (k_{app}) reported below are second-order rate constants for the hydrolysis and hydration reactions, obtained by dividing the observed rate constant obtained from first-order fits of substrate concentration versus time by the active catalyst concentration or, in the case of HPN hydration, directly from the GIT iterative kinetics fitting program. The details of the GIT models and an example fit are shown below. The active catalyst concentration, [cat.], was determined from the total molybdocene concentration using the appropriate equilibrium constants reported above. Because no monomer−dimer equilibrium was observed for the *ansa* catalyst, the total molybdocene concentration equals the active catalyst concentration.

Nitrile Hydration. Prior studies established the pathway in Scheme 1 for the hydration of nitriles catalyzed by molybdocenes.[3] It was also previously shown that the reactions are retarded by reversible coordination of the nitrile substrate (eq 6) and irreversible coordination of the amide product (eq 7), which leads to degradation of the catalyst.[3] Electron-withdrawing nitriles, however, exhibited increased catalytic activity with no product inhibition. Of the molybdocene-catalyzed hydrations reported earlier, the hydration of 3-hydroxypropionitrile (HPN) was the most efficient and was, therefore, chosen for this study. Although no product inhibition was noted with HPN, H/D exchange of the α-hydrogen atoms was observed (eq 8).

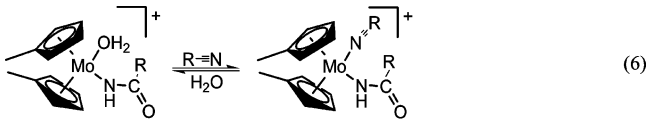

(6)

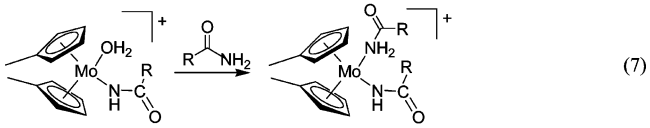

(7)

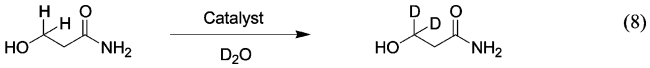

(8)

The reaction kinetics for nitrile hydration and product inhibition were modeled using an iterative kinetics fitting program (GIT) applied to eqs 9 and 10.

$$\text{catalyst} + \text{nitrile} \xrightarrow{k_{app}} \text{catalyst} + \text{amide} \qquad (9)$$

$$\text{catalyst} + \text{amide} \xrightarrow{k_2} \text{catalyst} + \text{amide-}d_2 \qquad (10)$$

An example of a fit is shown in Figure 7, and lists of the rate constants for 3-hydroxypropionitrile hydration (k_{app}) and H/D exchange (k_2) are shown in Table 5. The rate constants

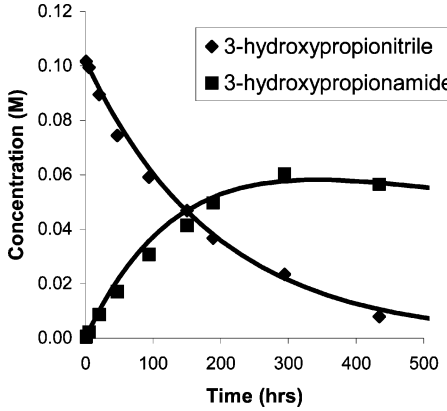

Figure 7. GIT fit of kinetics data for $C_2Me_4Cp_2Mo(OH)(OH_2)^+$-catalyzed hydration of 3-hydroxypropionitrile.

Table 5. Comparison of Kinetic Data for 3-Hydroxypropionitrile Hydration at 81 °C

ligand	[monomer] (mM)	[substrate] (M)	k_{app} (M^{-1} s^{-1} × 10^3)	k_2 (M^{-1} s^{-1} × 10^4)
$C_2Me_4(C_5H_4)_2$	1.2	0.10	1.2 ± 0.1	3.9 ± 0.3
$(C_5H_5)_2$	1.3	0.26	5.3 ± 0.7	5.1 ± 0.7
$(C_5H_4Me)_2$	1.8	0.092	4.3 ± 0.5	1.6 ± 0.2

for HPN hydration decrease in the order $Cp_2Mo(OH)(OH_2)^+ \sim Cp'_2Mo(OH)(OH_2)^+ > C_2Me_4Cp_2Mo(OH)(OH_2)^+$. The rate constants for H/D exchange give a slightly different trend than those for nitrile hydration, decreasing in the order $Cp_2Mo(OH)(OH_2)^+ \sim C_2Me_4Cp_2Mo(OH)(OH_2)^+ > Cp'_2Mo(OH)(OH_2)^+$. Although the trends for nitrile hydration and H/D exchange are intriguing, it should be noted that the variations in the rate constants for the three catalysts are only marginal. Such small changes in the rate constants for these catalysts show that the rate of nitrile hydration and H/D exchange is effectively unchanged for molybdocenes within the range of electron densities studied herein.

The sensitivity of HPN hydration to changes in electron density of the molybdocene catalyst may be reduced due to preferential coordination of the alcohol functionality of HPN as opposed to the nitrile group. Several observations indicate that HPN does in fact bind to the active site of the *ansa* catalyst through the alcohol functionality. Alcohol coordination was observed in the ^1H NMR spectrum of the reaction mixture by comparison of the aromatic Cp protons for the active catalyst to those of the catalyst in methanol/water mixtures (Figure 8). Note in the figure that the Cp resonances give two sets of pseudotriplets at essentially the same shift value (about 6.2 and 6.5 ppm in both cases). This result implies a similar ligand environment for each Mo atom. The complex in aqueous methanol must bind through the oxygen, and the implication therefore is that the HPN is bonded through the oxygen atom. In addition, H/D exchange of the α-hydrogens is observed over the course of the reaction, resulting in a decrease in intensity of the corresponding nitrile and amide resonances in the ^1H NMR spectrum. Molybdocene-catalyzed H/D exchange reactions in alcohols are known to proceed by initial coordination of the alcohol functionality.[6]

Phosphate Hydrolysis. The rate laws for phosphate hydrolysis using the molybdocene catalysts are pseudo-first-order, and a first-order fit of the kinetic data obtained using $Cp'_2Mo(OH)(OH_2)^+$ is shown in Figure 9. The rate constants are shown in Table 6. Comparison of these data to those in Table 5 shows

(48) Adams, M. A.; Folting, K.; Huffman, J. C.; Caulton, K. G. *Inorg. Chem.* **1979**, *18*, 3020−3.

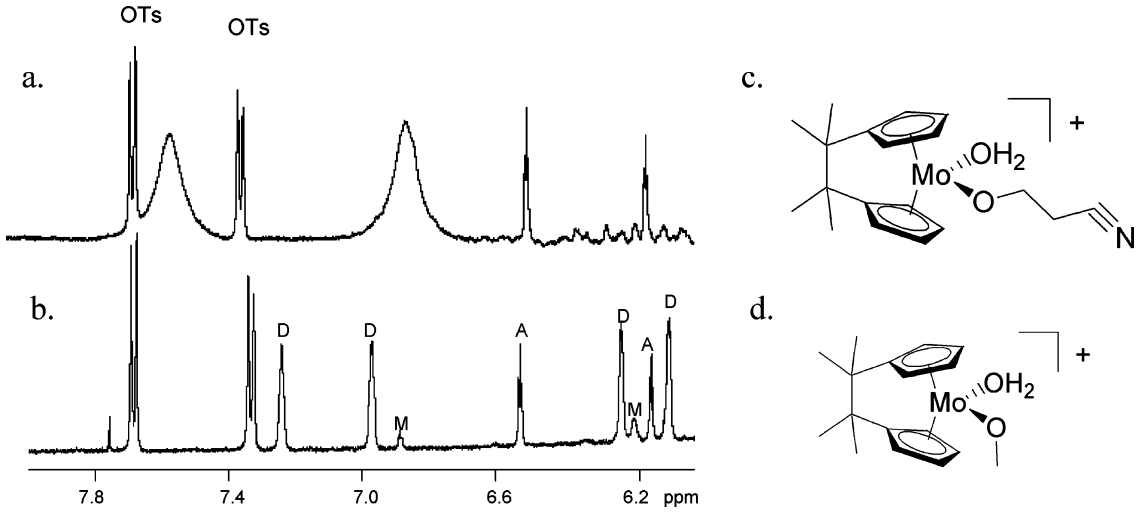

Figure 8. Aromatic regions of the ^{1}H NMR spectra of (a) a HPN hydration reaction mixture at 8 h and (b) the catalyst in a 1:1 water/methanol mixture. The proposed structures of (c) HPN coordination via the alcohol and (d) the *ansa*-molybdocene methanol adduct. OTs = C_6H_4Me, D = $[C_2Me_4Cp_2Mo(\mu\text{-}OH)]_2[OTs]_2$, M = $[C_2Me_4Cp_2Mo(OH)(OH_2)][OTs]$, and A = $[C_2Me_4Cp_2Mo(OCH_3)(OH_2)][OTs]$.

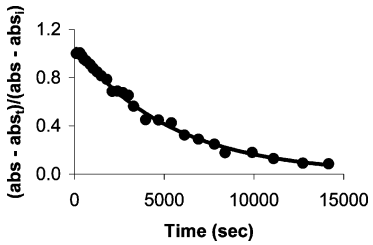

Figure 9. Kinetic data for hydrolysis of *p*-nitrophenyl phosphate promoted by $Cp'_2Mo(OH)(OH_2)^+$ fit to the exponential equation $y = 1.06e^{-1.87\times10^{-4}}$, $R^2 = 0.992$.

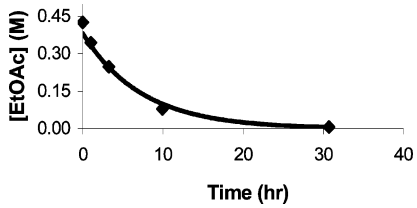

Figure 10. $Cp_2Mo(OH)(OH_2)^+$-catalyzed hydrolysis of ethyl acetate fit to the exponential equation $y = 0.382e^{-0.136}$, $R^2 = 0.994$.

Table 6. Comparison of NPP Hydrolysis Kinetics at 30 °C

ligand	[monomer] (mM)	k_{app} ($M^{-1}\,s^{-1} \times 10^2$)
$\{C_2Me_4(C_5H_4)\}$	0.50	1.6 ± 0.3
$(C_5H_5)_2$	0.80	64 ± 9
$(C_5H_4Me)_2$	3.8	5.3 ± 0.7

that the molybdocenes are more reactive toward phosphate substrates than nitriles; however, phosphate hydrolysis (eq 11) is not catalytic.[10] The enhanced rate may be due to the greater stability of the product P═O bonds relative to the C═O product bonds that form in the nitrile hydration reactions. The lack of turnover may be due to the greater stability of the four-membered Mo-phosphate structure in the product (eqs 12 and 13). Nevertheless, the hydrolysis of *p*-nitrophenylphosphate (NPP) was examined in order to further investigate the reactivity of the molybdocene molecules toward intramolecular nucleophilic attack.

As shown in Table 6, NPP hydrolysis was most efficient using the unsubstituted molybdocene catalyst $Cp_2Mo(OH)(OH_2)^+$, as the rate constants decrease in the order $Cp_2Mo(OH)(OH_2)^+ > Cp'_2Mo(OH)(OH_2)^+ > C_2Me_4Cp_2Mo(OH)(OH_2)^+$. These results support the hypothesis that the changes in the electronic environment are counteractive. In other words, the increase in activation of the substrate by the more electrophilic Mo center is offset by deactivation of the hydroxo leaving group. With the electron-donating Cp′ ligand, the increase in nucleophilicity of the hydroxo ligand is offset by the reduced reactivity of the substrate. It is interesting to note that phosphate ester hydrolysis is much more sensitive to alterations in the electronic environment of the metal center; the rate constant k_{app} is decreased by an order of magnitude as a result of an increase or decrease in the electron density of the Mo center as opposed to a factor of 4 or less in HPN hydration. In this case, changes in the electronics of the Mo center seem to affect the reactivity of the nucleophile and substrate to the same extent, leading to similar k_{app} values for $Cp'_2Mo(OH)(OH_2)^+$ and $C_2Me_4Cp_2Mo(OH)(OH_2)^+$.

Table 7. Comparison of Ethyl Acetate Hydrolysis Kinetics for Listed Molybdocenes at 80 °C

ligand	[monomer] (mM)	[EtOAc] (M)	k_{app} ($M^{-1}\,s^{-1} \times 10^{-3}$)
$\{C_2Me_4(C_5H_4)_2\}$	2.2	0.12	4.0 ± 0.2
$(C_5H_5)_2$	2.3	0.43	17 ± 1
$(C_5H_4Me)_2$	9.0	0.50	1.4 ± 0.3

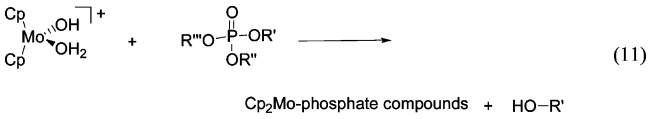

(11)

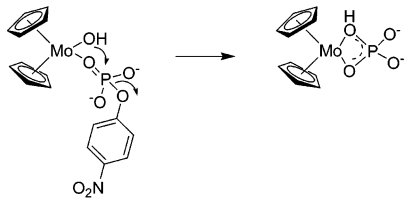

(12)

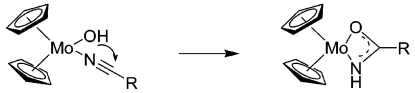

(13)

Carboxylic Ester Hydrolysis. The kinetic data for the hydrolysis of ethyl acetate are summarized in Table 7. Again, when comparing k_{app} values, the $Cp_2Mo(OH)(OH_2)^+$ catalyst

is an order of magnitude more reactive than the $C_2Me_4Cp_2Mo(OH)(OH_2)^+$ and $Cp'_2Mo(OH)(OH_2)^+$ catalysts. As with the other catalytic reactions, this trend suggests that $Cp_2Mo(OH)(OH_2)^+$ has optimal electron density on the metal center for reactions proceeding by intramolecular nucleophilic attack.

Effect of Monomer−Dimer Equilibrium on the Reaction Rate. The formation of an inactive dimeric species was found to be of critical importance in determining the reaction rates for the Cu(II) macrocyclic amine phosphate ester hydrolysis catalysts reported by Burstyn and co-workers.[32] The Cu(II)-promoted hydrolysis reactions were shown to exhibit a half-order dependence on the total Cu(II) concentration, and the active catalyst was proposed to be a monomer that exists in equilibrium with a dimer (eq 14), analogous to the monomer−dimer equilibrium observed with the molybdocene catalyst (eq 1). In an investigation of the effect of ligand structure on reactions rates in the Cu(II) system, Burstyn and co-workers found that the rate of hydrolysis increased with increasing ligand size due to a resulting destabilization of the inactive dimeric species. Other factors such as the Lewis acidity of the Cu(II) center and steric constraints on the phosphate binding were also proposed to have an affect on the reaction rates but were concluded to be of secondary importance.

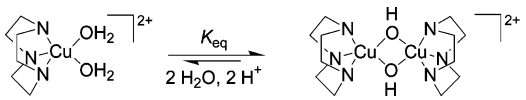

(14)

Because of the monomer−dimer equilibrium in eq 1, the rates of hydrolysis and hydration can be similarly affected by dimerization in the non-*ansa* catalysts, especially in the case of nitrile hydration, where changes in the electronics of the metal center resulted in the smallest variations in rate constants. Accordingly, although the unsubstituted $Cp_2Mo(OH)(OH_2)^+$ catalyst is the most reactive toward intramolecular nucleophilic attack, the *rate* of $Cp_2Mo(OH)(OH_2)^+$-catalyzed hydration and hydrolysis reactions per *total* molybdenum concentration may not be fastest due to the extensive dimer formation. Note that because the $C_2Me_4Cp_2Mo(OH)(OH_2)^+$ catalyst is not in apparent equilibrium with a dimeric species, the actual rate of hydration or hydrolysis per mole of total Mo(IV) may be increased for the *ansa* catalyst. Further studies on the effect of catalyst dimerization in these molybdocene systems are underway in our laboratory.

Summary and Key Insights

A major goal in homogeneous catalysis is identifying specific ligand sets that afford selective catalytic transformations of organic substrates with maximum turnover rates. Molybdocenes have outstanding selectivity and moderate reactivity in the hydration of nitriles in aqueous solution, and they display promise in phosphate ester degradation. In an effort to explore the reactivity of a more electrophilic molybdenum center toward hydrolysis and hydration reactions, the tetramethylethylene-bridged bis(cyclopentadienyl) ligand was employed. The ethylene bridge was shown to alter the molybdocene catalyst in three significant ways. First, the ethylene bridge greatly reduced the water solubility of the catalyst. Second, the bridging ring substituents suppressed formation of the inactive μ-hydroxo dimer. Third, the ethylene bridge increased the electrophilicity of the molybdenum center, as shown by the relatively high energy $\nu(C{\equiv}O)$ stretching frequency in $C_2Me_4Cp_2Mo(CO)H$ compared with the analogous non-*ansa*-molybdocenes studied herein.

Although the *ansa* linkage reduced the electron density at the Mo center, the increase in the Lewis acidity did not increase the reactivity of a bound substrate toward intramolecular nucleophilic attack by the hydroxo ligand. In fact, the observed trends in the rate constants did not correlate with the electron density on the metal center. Instead, the $Cp_2Mo(OH)(OH_2)^+$ catalyst, which has intermediate electron density, was the most reactive toward every substrate examined. These results were interpreted by evaluating the competing effects of changes in the electrophilicity of the Mo center, namely, that an increase in the electrophilicity will increase the reactivity of a bound substrate toward nucleophilic attack but will also decrease the reactivity of the bound hydroxo nucleophile.

Acknowledgment is made to the NSF for the support of this research. T.J.A. would also like to acknowledge the Haugland Fellowship for partial support.

Supporting Information Available: Crystallographic data for **2**, **5**, and $[\{C_2Me_4(\eta^5\text{-}C_5H_4)_2\}Mo(\mu\text{-}OH)]_2[OTs]_2{\cdot}2H_2O$ and details of the data collections and refinements of the crystal structures. The ^1H and ^{13}C NMR spectra for synthetic intermediate **2**. This material is available free of charge via the Internet at http://pubs.acs.org.

OM7004657